

Non-chain superstructures of $\text{YBa}_2\text{Cu}_3\text{O}_{6.375}$ at finite temperatures

This article has been downloaded from IOPscience. Please scroll down to see the full text article.

1995 J. Phys.: Condens. Matter 7 7253

(<http://iopscience.iop.org/0953-8984/7/36/014>)

View [the table of contents for this issue](#), or go to the [journal homepage](#) for more

Download details:

IP Address: 171.66.16.151

The article was downloaded on 12/05/2010 at 22:05

Please note that [terms and conditions apply](#).

Non-chain superstructures of $\text{YBa}_2\text{Cu}_3\text{O}_{6.375}$ at finite temperatures

P J Kundrotas^{†‡}, E E Tornau^{†§} and A Rosengren[†]

[†] Department of Physics/Theoretical Physics, The Royal Institute of Technology, S-100 44 Stockholm, Sweden

[‡] Faculty of Physics, Vilnius University, Saulėtekio 9, 2054 Vilnius, Lithuania

[§] Semiconductor Physics Institute, Goštauto 11, 2600 Vilnius, Lithuania

Received 14 February 1995, in final form 1 June 1995

Abstract. The possible existence of non-chain superstructures in $\text{YBa}_2\text{Cu}_3\text{O}_{6.375}$ is studied by Monte Carlo simulation in the framework of the lattice gas model with screened Coulomb potential pair interactions. It is found that this model is capable of describing the occurrence of such structures only if the interactions are cut off at a certain distance. Then, only the superstructure proposed from the neutron diffraction experiments of Sonntag *et al* is found to be stable at finite temperature. A phase diagram with coexisting chain, non-chain and disordered structures is obtained.

1. Introduction

Studies of the oxygen subsystem in $\text{YBa}_2\text{Cu}_3\text{O}_{6+x}$ demonstrate that the oxygen atoms form O–Cu–O chains in the CuO_x plane of this compound. The compound becomes orthorhombic at $x > 0.4$, and chain formation results in the creation of the stable orthorhombic phases O_I , with stoichiometry $x = 1$, and O_{II} , with stoichiometry $x = 0.5$ (see [1, 2]). Other orthorhombic superstructures with copper–oxygen chains, observed as small domains by electron diffraction [1, 3] or by electron microscopy [4] at oxygen stoichiometries in between those of the main two phases, are interpreted as stable [5, 6], transient [7] or metastable [8]. In view of the most recent x-ray diffraction results [9, 10], the cell-tripled O_{III} phase is, probably, the only stable phase among them (see also [11, 12, 13]).

Despite the fact that the structures of $\text{YBa}_2\text{Cu}_3\text{O}_{6+x}$ conventionally are described in terms of copper–oxygen chains, some interpretations of diffraction experiments favour one or another non-chain superstructure. Usually these superstructures are observed at low oxygen concentrations and in quenched samples. At an early stage of the investigations of $\text{YBa}_2\text{Cu}_3\text{O}_{6+x}$ such superstructures were proposed by Alario-Franco *et al* [14] on the basis of x-ray diffraction results. Later such superstructures were observed in samples heated in the vacuum of an electron microscope [4, 15]. The most recent non-chain structures were proposed in [16] from neutron and x-ray diffraction experiments on a non-superconducting sample, of oxygen amount around $x = \frac{3}{8}$. The $2\sqrt{2} \times 2\sqrt{2}$ and $2\sqrt{2} \times \sqrt{2}$ structures were obtained in a tiny region of oxygen concentration, known as the border between the tetragonal and orthorhombic structures, on one hand, as well as the border between the semiconducting and metallic properties, on the other.

The proposed non-chain structures were unexpected to most theorists as well. Usually the ASYNNNI model [17] is successfully employed for the description of the tetragonal to orthorhombic phase transition in $\text{YBa}_2\text{Cu}_3\text{O}_{6+x}$. The main ingredients of this model are the repulsion between nearest-neighbour oxygen atoms (effective interaction constant $v_1 > 0$), the attraction between second-nearest-neighbour oxygen atoms separated by copper ($v_2 < 0$), which stabilizes the copper–oxygen chains, and the repulsion between second-nearest-neighbour oxygen atoms without a copper atom in between ($v_3 > 0$). This model is adequate for the description of the main orthorhombic phases, O_I and O_{II} , both in $\text{YBa}_2\text{Cu}_3\text{O}_{6+x}$ and in another member of the same family of compounds, $\text{Y}_2\text{Ba}_4\text{Cu}_7\text{O}_{14+x}$ [18, 19]. To stabilize other long-period chain structures, e.g. O_{III} , an additional longer-range repulsive interaction is needed [11, 12]. However, the non-chain structures of [16] cannot be stabilized when the interaction between the second-nearest-neighbour oxygen atoms separated by copper is attractive (unless the initial model is modified to include strain effects [20, 21, 22]). Another model was proposed by Aligia *et al* [23, 24, 25]. Screened Coulomb interactions between the oxygen atoms, and a repulsive second-nearest-neighbour oxygen interaction, mediated by copper ($v_2 > 0$), were the main features of this model. A positive v_2 is needed to make the non-chain structures stable. It should be noted though, that the studies [23, 24, 25] were restricted to zero temperature.

The main arguments of the discussion between the authors of the two models about the nature of the effective interaction potential along the chains, v_2 , are summarized below.

In view of the strong Cu–O attraction, caused by the Cu d orbital and the O p orbital covalency, threefold Cu coordination (chain ends, O–Cu–v) was claimed [6] to be highly unfavourable in comparison to twofold (v–Cu–v) and fourfold (O–Cu–O) Cu coordinations (here v stands for an oxygen vacancy in the chain). This claim was confirmed by first-principles calculations [26, 27] demonstrating the interaction constant v_2 to be attractive. On the other hand, Aligia and Garces [28] performed a calculation on the extended Hubbard model for the copper–oxygen subsystem in the absence of charge transfer ($x < 0.5$) in two cases, where the model can be solved exactly. The result was that the energy of the system arranged in infinite O–Cu–O chains is higher than the energy of the system without first- and second-nearest-neighbour oxygen atoms. In the ASYNNNI model this difference is proportional to v_2 . Hence it was concluded that the sign of v_2 cannot be determined without performing a more elaborate calculation [28]. This conclusion was questioned in [29]. The isolation of the copper–oxygen subsystem from other atoms in real $\text{YBa}_2\text{Cu}_3\text{O}_{6+x}$ as well as the neglect of the extremely large elastic energies, changing the contribution of the Hubbard model to the formation energy, were pointed out as the main deficiencies of the approach chosen. It should be noted, however, that these deficiencies could be attributed to every simple model and to the original ASYNNNI model [17] as well.

In this paper the model with screened Coulomb potentials is used to perform a Monte Carlo study of superstructures appearing in $\text{YBa}_2\text{Cu}_3\text{O}_{6+x}$ at $x = \frac{3}{8}$. Since a controversy on the relevance of the model chosen exists, we analyse whether its application leads to serious contradictions. We find that this model is capable of describing the occurrence of non-chain structures at the oxygen stoichiometry considered *only if* the interactions are cut off at a certain distance. From an analysis of the superstructures appearing at different cut-offs of the interactions we show which of these superstructures, proposed in [16, 23, 24, 25], is stable at finite temperature in this model. Finally, we study the thermodynamic properties of the superstructure obtained and present the phase diagram with the chain, non-chain and disordered phases included.

2. Model and phases

For our calculations we use the model [23] in which the oxygen atoms in the CuO_x plane repel each other by a screened Coulomb interaction. The interaction between two oxygen atoms, separated by a copper atom, is varied by means of a coefficient f , which can be either positive or negative. The lattice gas Hamiltonian is expressed as

$$\mathcal{H} = \sum_{i \neq j} v_{ij} n_i n_j - \mu \sum_i n_i \quad (1)$$

where n_i is the occupancy number equal to one or zero, depending on the site i being occupied by an oxygen atom or not, and μ is the chemical potential. The interaction constants depend on the distance between the oxygen atoms in the following manner

$$v_{ij} = \frac{v_{10}}{|R_i - R_j|} \exp \left\{ -\frac{|R_i - R_j|}{\lambda} \right\} \quad (2)$$

but in the case of interaction with a copper atom in between

$$v_{ij(\text{over Cu})} = f v_{ij}. \quad (3)$$

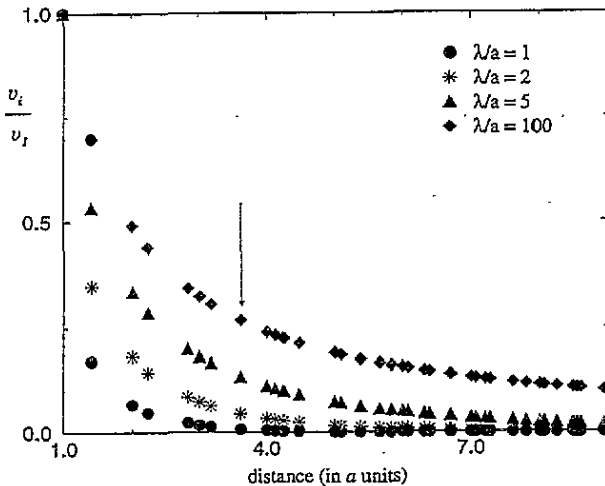


Figure 1. The decay of the magnitude of the interaction potentials for the model (2) at $f = 1$. The arrow indicates the cut-off distance $a\sqrt{13}$ at which the N phase occurs.

Here λ is the screening length, and v_{10} is the unscreened nearest-neighbour interaction constant, which is estimated to be equal to about 1 eV [24]. The magnitude of v_{ij} at different values of λ/a , where $a = a_0/\sqrt{2}$ and a_0 is the lattice constant, is presented in figure 1. At small values of λ and $f < 0$ the model (1)–(3) is reduced to the ASYNNNI model. It should be noted that the model (1)–(3) with long-range interactions for finite temperatures and negative values of f was studied in [30], where a complete devil's staircase of phases with different arrangement of O–Cu–O chains was obtained. Here we explore the case $f > 0$.

Four candidates for the stable non-chain superstructure at the stoichiometry $x = \frac{3}{8}$ have been suggested on the basis of neutron diffraction results [16] and theoretical studies at zero temperature with $f > 0$ [23, 24], in which a ground state analysis was performed with some restrictions on the size of the unit cell. Hereafter, we shall use the notations N, Q,

R, and G for these phases (the oxygen arrangements within the unit cell of each phase are shown as insets to figure 2).

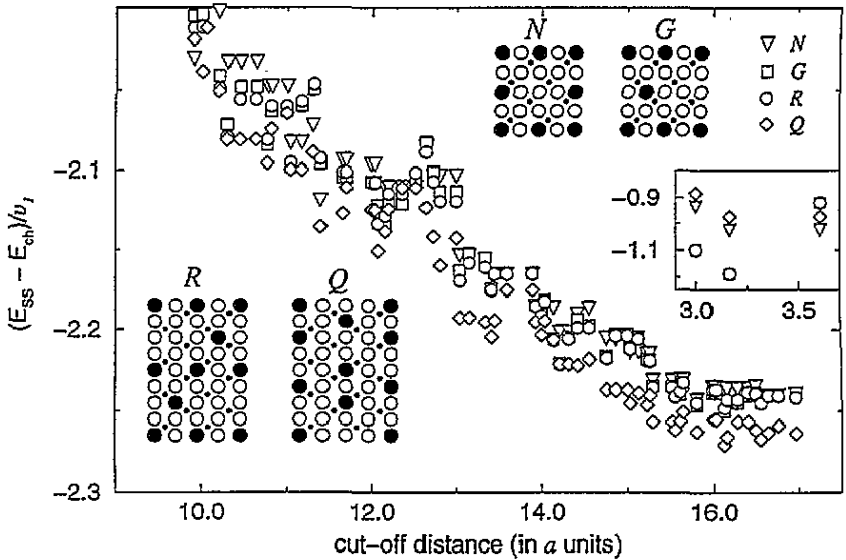


Figure 2. The difference in energies at temperature $T = 0$ between the superstructures N, Q, R, G and the chain structure for the stoichiometry $x = \frac{3}{8}$, as a function of the cut-off of the interaction at $f = 1, \lambda/a = 5$. This function in the vicinity of the cut-off of the interaction $a\sqrt{13}$ is shown as inset. The corresponding non-chain superstructures are also shown as insets. Small solid circles denote copper, large solid circles—oxygen atoms and large open circles—oxygen vacancies.

Since $\text{YBa}_2\text{Cu}_3\text{O}_{6+x}$ is semiconducting at $x = \frac{3}{8}$, the screening of the interactions in (2) has to be rather weak, and λ has to exceed a notably. Hence, in general, one should keep a large number of interaction constants in the Hamiltonian (1), at least up to the range where addition of new interaction constants does not change the ground state energy significantly. To determine this range we have performed calculations of the energies at zero temperature for the N, Q, R, and G phases. The results for $\lambda/a = 5$ are shown in figure 2. Each set of energy values at a certain range in this figure means that the energies were calculated with the interaction truncated at this range. It is seen that there exists a certain distance a_c above which the addition of more interactions does not affect the energies of the phases considered. This distance increases significantly with increasing λ/a ($a_c = 8a$ for $\lambda/a = 2$, and $a_c = 16a$ for $\lambda/a = 5$). Due to this rapid increase, we were only able to perform Monte Carlo studies for the model (1) with infinite interaction range for values of λ/a up to 5. Note that the Q phase has the lowest energy of the four phases studied in accordance with [24].

The Monte Carlo calculations were performed using Glauber dynamics (non-conserved number of particles) on a square lattice $L \times L$ ($L = 40$) with periodic boundary conditions. To see whether the results of our simulation are influenced by finite-size effects, we also performed calculations on larger lattices for the interaction cut-offs of special interest (e.g. $a\sqrt{13}$, see below) up to $L = 320$. The obtained entities were averaged over 5000–10 000 MCS/site after the system reached equilibrium.

The curve to the right in figure 3(a) shows the $x(\mu)$ dependence obtained at $\lambda/a = 5$ and at the temperature $t = T/v_1 = 0.03$ which corresponds to room temperature. Here

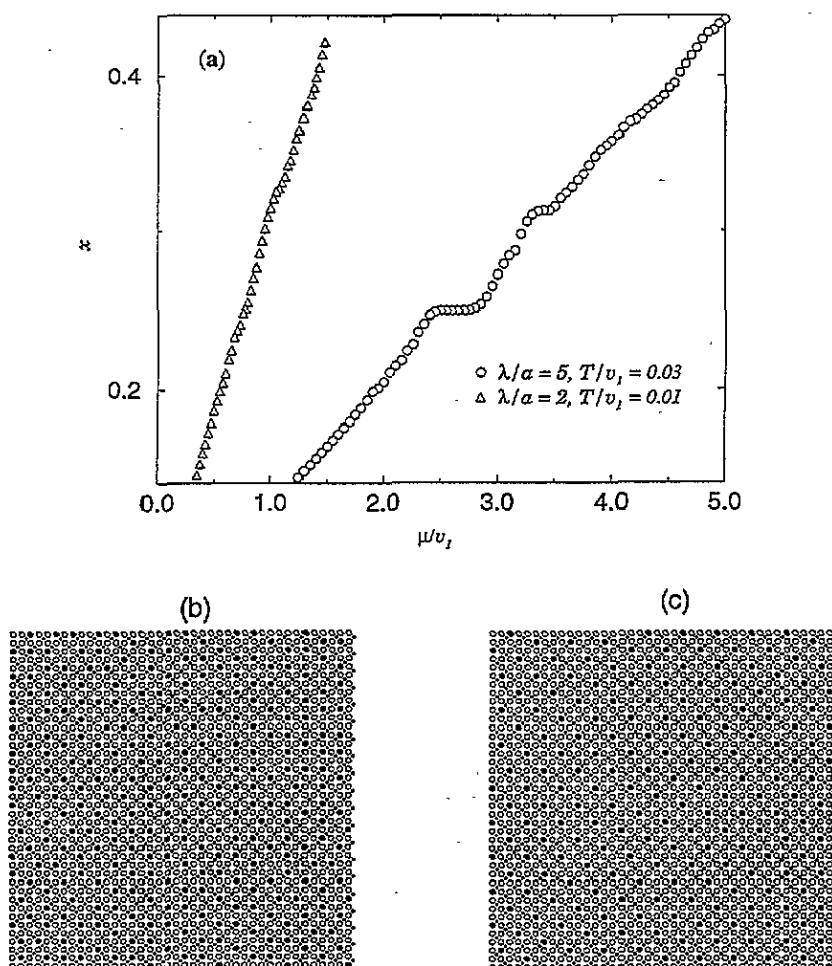


Figure 3. Dependence of the oxygen amount x on the chemical potential for $f = 1$ at various values of the screening parameter λ/a and the temperature T/v_1 (a) and snapshots of the oxygen arrangement at $\lambda/a = 5$, $T/v_1 = 0.03$ and $x = \frac{3}{8}$ (b) and $x = 0.25$ (c). The notation for the snapshots are the same as for the insets to figure 2.

we have taken into account interactions up to distance $17a$ which exceeds the estimated a_c for this value of λ/a . The $x(\mu)$ dependence does not exhibit any plateau at $x = \frac{3}{8}$ which would indicate a stable ordered structure at finite temperatures. The snapshot of the oxygen arrangement at this stoichiometry also does not show any traces either of the Q phase or of the N, G, and R phases (see figure 3(b)). On the other hand, there are two plateaus at lower x . The plateau at $x = 0.25$ corresponds to an ordered structure with the unit cell $2a\sqrt{2} \times 2a\sqrt{2}$ (see figure 3(c)). The structure at $x = 0.32$ (where another plateau in $x(\mu)$ is observed) represents the structure at $x = 0.25$ with every second half-empty O-Cu-O chain distorted due to the presence of additional oxygen atoms. Note that our results for $\lambda/a = 2$, also shown in figure 3a (in this case we have included interactions up to $9a$), do not show any ordering down to $t = T/v_1 = 0.01$ at any x considered.

All the calculations mentioned above are restricted to the case when there is no reduction of the interactions due to the presence of Cu atoms in between the oxygen atoms ($f = 1$).

Among the four non-chain phases considered, the N phase contains the largest number of oxygen atoms interacting via Cu atoms. Hence, this reduction may play a significant role for stabilizing the N phase. Therefore we have performed MC calculations at $\lambda/a = 5$ for various f values. Our results do not differ from those at $f = 1$ down to $f \sim 0.85$. Below this value we observe a plateau in the $x(\mu)$ dependence at $x = \frac{3}{8}$. This plateau corresponds to a phase with alternating filled, empty and half-filled O–Cu–O chains. For $f \lesssim 0.5$ we observe the usual chain structure.

On the basis of these calculations we conclude that the model with infinite interaction range cannot describe the existence of non-chain structures (neither the superstructures Q or N nor any other superstructures in $\text{YBa}_2\text{Cu}_3\text{O}_{6+x}$ at $x = \frac{3}{8}$). Therefore instead the truncated model (1), (2) was studied in order to answer these questions: how many interactions should be kept in the Hamiltonian (1) to obtain the structure observed in experiment [16] and which of the phases proposed in [24] is stable at finite temperatures? Our choice of such a truncated model is rather artificial, but is the only possibility to obtain these superstructures (within the model of general form considered). It should be noted that a cut-off of the interactions is characteristic to studies of numerous systems in condensed matter physics. Even for $\text{YBa}_2\text{Cu}_3\text{O}_{6+x}$ a truncation of the interactions at the fourth interaction constant is used in the extended ASYNNNI model [11, 12], which is used for studying the properties of the orthorhombic O_{III} phase. A ground state analysis (see inset to figure 2) and Monte Carlo calculations at low temperatures demonstrate the N phase to be stable in a wide region of λ/a values (from two up to 100) when the interactions are truncated at the distance $a\sqrt{13}$ (this means that 10 interaction constants must be taken into account). This phase does not appear either at low or at higher temperatures with any other cut-off.

The Q phase, which was proposed in [24] to be the most probable superstructure in $\text{YBa}_2\text{Cu}_3\text{O}_{6.375}$, occurs in some of our runs at large values of λ/a (~ 100), when 13 interaction constants are kept (up to $\sqrt{18}a$). However, in most cases the phase $\sqrt{5} \times \sqrt{5}$ with the close stoichiometry $x = 0.4$ prevails instead. Due to this competition and due to the large hysteresis in the $x(\mu)$ dependence between these two phases, we have performed a special analysis which demonstrated that the superstructure Q is a metastable phase, at least down to the temperature $t = T/v_1 \geq 0.01$, where we still could obtain reliable results.

Accounting also for some other cut-offs, we observe some other superstructures with stoichiometry $x = \frac{3}{8}$ which were not considered in the ground state analysis [23, 24]. One of them is a superstructure with the unit cell (figure 4c) four times as large as that of the N phase. This phase appears when 11 interaction constants are kept (up to $4a$). Another phase was found when interactions of range $a\sqrt{29}$ were kept (figure 4d). This phase is an example of the ‘exotic’ phases sometimes observed in our calculations for the cut-offs exceeding $a\sqrt{18}$. For *all other* cut-offs no plateau is observed in the $x(\mu)$ dependence at $x = \frac{3}{8}$. This indicates that the system is either disordered or decomposed, or that other phases with slightly higher stoichiometry are present at $x = \frac{3}{8}$. Thus, we conclude that out of the four candidates for the stable non-chain superstructure [16, 23, 24] only the superstructure N which was suggested from the neutron diffraction experiment [16] can be described in the framework of Hamiltonian (1) with a finite number of interaction constants taken into consideration.

3. Thermodynamical properties of the N superstructure

Using the set with 10 interaction constants, we performed a simulation in order to determine the stability limits of the N phase in the coordinates (T, f) . The phase diagram obtained is

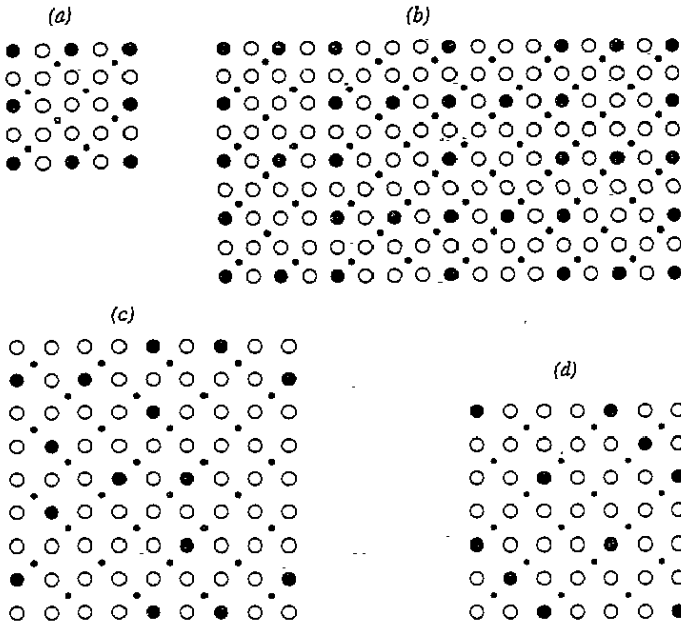


Figure 4. The superstructures appearing in calculations at $x = \frac{3}{8}$: (a) N; (b) 'dislocated' N; (c) unit cell of a superstructure observed for a cut-off at $4a$; (d) at $a\sqrt{29}$.

presented in figure 5. The phase transition between the chain and the disordered structure was determined from the position of the peaks either in the temperature dependence of specific heat $C(T)$ or in the f dependence of the susceptibility $\chi(f)$, which are related to the fluctuations of the energy and equilibrium stoichiometry x of the system, respectively. The location of the transition to the N structure was determined from the midpoint in the $x(T)$ or $x(f)$ hysteresis. Since the hysteresis is weak (see figure 6(a)), the error in determining the transition point in this way is small. The transitions between the chain phase with some additional atoms between the chains, the N phase and the disordered phase are clearly indicated. The area of the N phase shrinks with decreasing screening length. This is seen from figure 6(a), where the temperature of the transition to the N phase decreases with decreasing λ/a . On the other hand, the width of the plateau in the $x(\mu)$ dependence corresponding to the N phase decreases with decreasing λ/a (see figure 6(b)), also indicating the narrowing of the stability region for the N phase. It also follows from figure 6(a) that the phase transition between the N phase and the high-temperature disordered phase, consisting of short O-Cu-O chains, is of the first order and, probably, close to being of the second order due to the weak hysteresis and the smooth form of the curves just below the transition point. The phase transitions between the chain and disordered structure are of the second order, and the transitions between the chain and the N phase are of the first order.

It should be noted that for some temperature and f sections the results were checked on some other lattices ($L = 39$ and 60). The N phase occurred in the phase diagram at the interaction cut-off at the range $a\sqrt{13}$ independently of lattice size; the shapes of the curves, used for the determination of the nature and location of the transitions do not change relative to that of 40×40 , and the transition points remain within the error bars shown in figure 5.

It is seen from figure 6(b) that the N phase can be formed by taking away the central

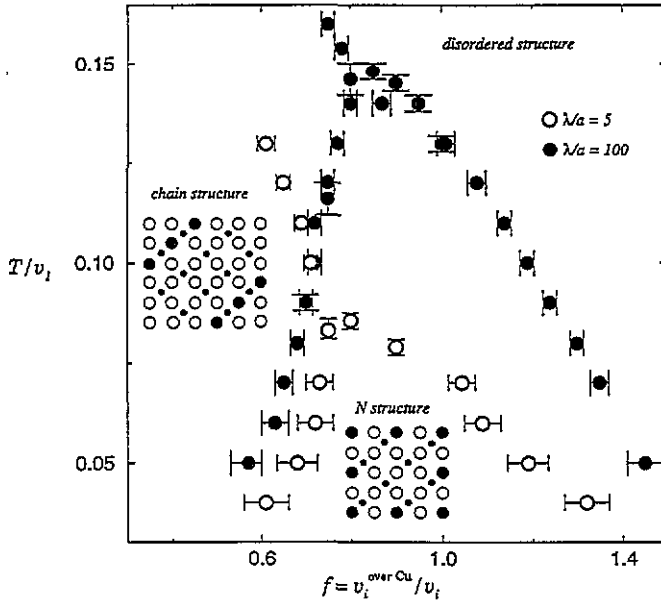


Figure 5. Phase diagram for $x = \frac{3}{8}$ at $\lambda/a = 5$ and 100. Error bars indicate the accuracy due to the width of the hysteresis for the first order phase transitions and the accuracy in determining the peaks for the second-order phase transitions.

atom from the unit cell of the phase, which we call N^+ (stoichiometry $x = 0.5$), or by adding one atom to the unit cell of the phase N^- (stoichiometry $x = 0.25$). Taking this into account, we constructed the order parameter for the N phase in the form

$$\eta_N = \sum_i (n_{1i} + n_{3i} - n_{2i} - n_{4i}) \quad i = a, b, c, d. \quad (4)$$

Here we used the notation of sites from figure 7, in which the f dependence of the order parameter η_N is also presented. Again, the first-order jump is clearly seen in the f dependence of η_N (such a jump is also found for the temperature dependence of η_N). Note that, at $t = T/v_1 = 0.06$, the order parameter saturates at lower values. This is due to the displacement of two neighbouring blocks with unit cell of the N structure by $2a$ with respect to the two other blocks, an effect (see figure 4(b)) often observed at higher temperatures.

4. Discussion

In our study we tried to answer the question of whether non-chain ordered superstructures of $YBa_2Cu_3O_{6.375}$, suggested from neutron diffraction experiments and a ground state analysis, can be described in the framework of the model with screened repulsive Coulomb interactions. Our answer is negative in the sense that this model with an infinite range of pair interactions cannot describe non-chain superstructures (at finite temperatures), either the ground state superstructure suggested, or any other ordered phase at $x = \frac{3}{8}$. Therefore instead we turned our attention to the truncated model. Only the N superstructure, proposed from neutron diffraction experiments [16], is stable at the stoichiometry $x = \frac{3}{8}$ (for cut-off at $a\sqrt{13}$). All other cut-offs result in no stable ordered structure being observed at this

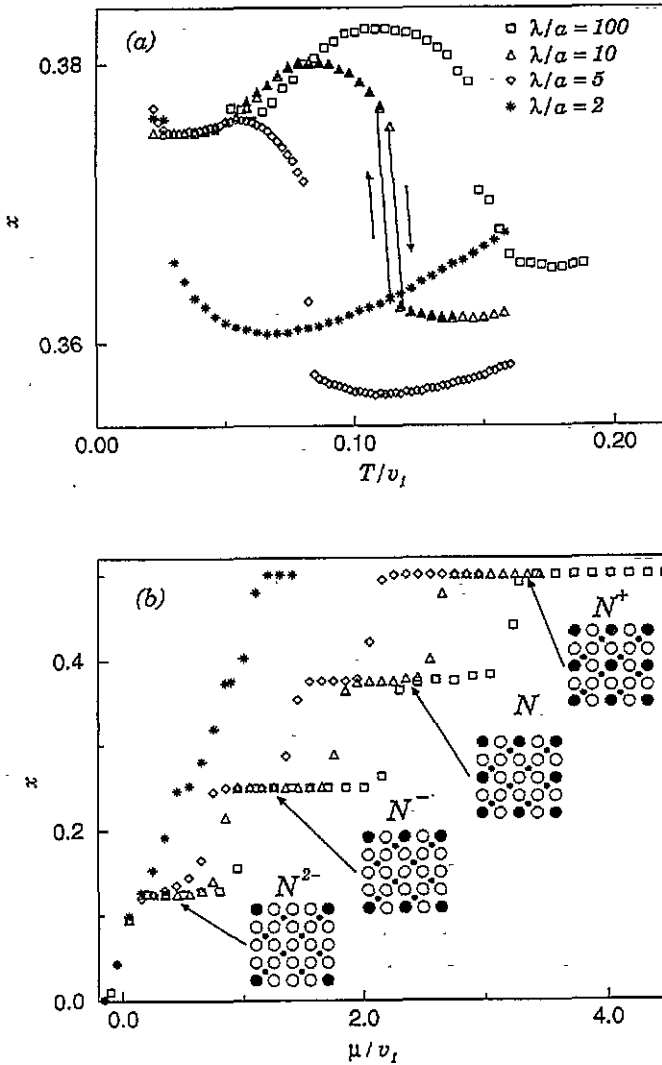


Figure 6. Dependence of the oxygen amount x on temperature (a) and the chemical potential at $t = T/v_t = 0.02$ (b) at different values of λ/a and $f = 0.8$ corresponding to the maximum of the N phase. The superstructures, responsible for the corresponding plateaus, are shown in the insets of (b). Narrow hysteresis, observed in all curves of (a), is shown only for $\lambda/a = 10$ for simplicity. The data for (a) are obtained at μ values corresponding to the midpoint of the plateau in (b).

stoichiometry (except for some exotic phases obtained for very large cut-offs). We have calculated the phase diagram for this truncated model and determined the stability region of the non-chain superstructure obtained with respect to both the chemical potential (which is related to the partial oxygen pressure in the experiments) and the reduction factor f of the model. It should be noted that the cut-off of interactions is rather artificial from the physical point of view, but it was the *only* possibility to obtain ordered structures, and especially the N superstructure, observed in experiments [16], in the framework of the lattice gas model with pair interactions, a model which is commonly accepted to be efficient in describing

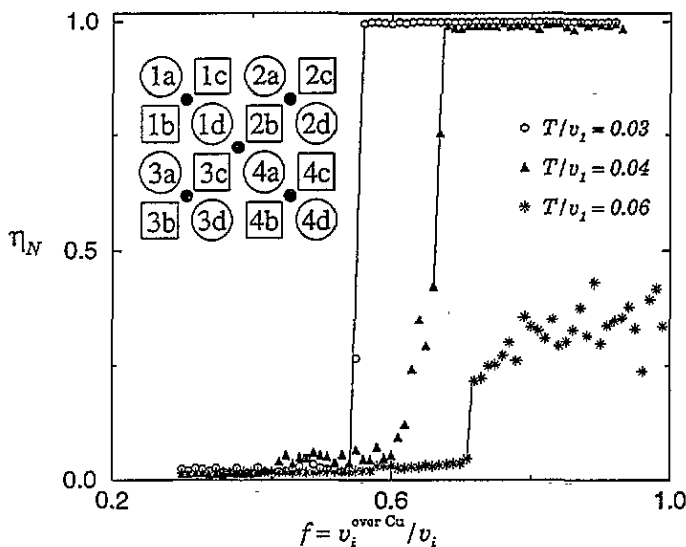


Figure 7. Dependence of the order parameter η_N on f for three values of the temperature, at $\lambda/a = 5$. Hysteresis is not shown, but it is observed for all cases ($\Delta f = 0.15$ for $T/v_1 = 0.04$). The enumeration of the oxygen sites for formulae (4) is given in inset.

phenomena related to the oxygen subsystem in $\text{YBa}_2\text{Cu}_3\text{O}_{6+x}$. Hence our analysis of the thermodynamic properties of the N phase should be considered only as qualitative.

Disordered ($x < 0.4$) or chain ($x > 0.4$) structures prevail when the samples are well prepared and unquenched. For the description of such samples, the ASYNNNI model is quite sufficient. Non-chain structures are a characteristic feature of quenched samples. In our model chain and non-chain structures coexist at positive values of $f = v_2/v_3$ (in the notation of the ASYNNNI model). In that sense this parameter might be related to the quality of the sample. It is known, for example, that vacancies are present at copper sites in the CuO_x planes of $\text{YBa}_2\text{Cu}_3\text{O}_{6+x}$. In those samples of $\text{Y}_2\text{Ba}_4\text{Cu}_7\text{O}_{14+x}$ which are characterized by low superconducting temperatures and misorientation of the O-Cu-O chains, vacancies are found at about 25% of the copper atom sites in that plane [31]. Thus, accordingly, some of the attractive constants v_2 of the ASYNNNI model have to be replaced by repulsive v_3 constants. This results in a shift of the whole region of the O_{II} phase in the (T, x) diagram towards smaller values of x and a turning of the chains around the copper vacancies [19]. The existence of copper site vacancies does not affect the chain structures at oxygen amounts close to the stoichiometry of the phases O_I or O_{II} , but it can be important in a tiny region close to the orthorhombic to tetragonal phase transition, where the non-chain structures are actually observed. In the phase diagram, calculated by the cluster variation method, quite large areas of decomposed phases are found between the tetragonal and O_{II} phases [32] comprising the concentration $x = \frac{3}{8}$. In this region metastable structures, consisting of short O-Cu-O chains directed along both axes, were proposed [6] as an explanation of the experimentally observed non-chain structure [16]. However, the superstructure reflections of the oxygen distribution in several randomly chosen places of this region, obtained by using the ASYNNNI model ($f < 0$), show a worse agreement with experiment than e.g. the superstructure N. Anyway, the idea of metastable phases is very attractive, though it is not clear how this structure can appear as an ordered pattern. In that sense the results of our simulations can be considered as another extreme: we obtain the

ordered structure from the artificially truncated model and cannot motivate unambiguously the choice of the v_2 sign.

A recent Monte Carlo simulation of deformation structures, caused by strain effects [20], seems to be a promising attempt to explain the appearing $2\sqrt{2} \times 2\sqrt{2}$ structures. The result is obtained for the completely ordered compound at $x = 1$. Calculations for oxygen amounts, corresponding to the region of the tetragonal-to-orthorhombic phase transition, would probably require long time scales and lead to very slow kinetics, but such a result in this case too would be evidence that the concept of strain prevails over the concept of oxygen ordering due to long-range interactions. However, the experiments with infinite-layer superconductors make an explanation in terms of strain [20] ambiguous: it was recently shown [33] that the $2\sqrt{2} \times 2\sqrt{2}$ structure appears in the infinite-layer superconductor when heated by an electron microscope, the same effect that was observed earlier by Krekels *et al* in $\text{YBa}_2\text{Cu}_3\text{O}_{6+x}$ [15]. It is well known, however, that these infinite-layer superconductors have no CuO_x planes at all.

Acknowledgments

We are grateful to A A Aligia and S Lapinskas for discussions. This work was supported by the Royal Swedish Academy of Sciences and by the Swedish Institute, and made possible in part by grant No LHT 100 from the International Science Foundation.

References

- [1] Werder D J, Chen C H, Cava R J and Batlogg B 1988 *Phys. Rev. B* **37** 2317; **38** 5130
- [2] Tornau E E, Lapinskas S, Rosengren A and Matic V M 1994 *Phys. Rev. B* **49** 15 952
- [3] Beyers R, Ahn B T, Gorman G, Lee V Y, Parkin S S, Ramires M L, Roche K P, Vazquez J E, Gür T M and Huggins R A 1989 *Nature* **340** 619
- [4] Reyes-Gasga J, Krekels T, Tendeloo Van G, Landuyt Van J, Bruggink W H M, Verweij H and Amenlinckx S 1989 *Solid State Commun.* **70** 269.
- [5] de Fontaine D, Mann M E and Ceder G 1989 *Phys. Rev. Lett.* **63** 1300
de Fontaine D, Ceder G and Asta M 1990 *Nature* **343** 544
- [6] de Fontaine D, Asta M, Ceder G, McCormack R, and Van Tendeloo G 1992 *Europhys. Lett.* **19** 229
- [7] Burmester C P and Wille L T 1989 *Phys. Rev. B* **40** 8795
- [8] Khachatryan A G and Morris J W Jr 1987 *Phys. Rev. Lett.* **59** 2776; 1988 *Phys. Rev. Lett.* **61** 215
- [9] Plakhty V, Stratilatov A, Chernenkov Yu, Fedorov V, Sinha S K, Loong C K, Gaulin B, Vlasov M and Moshkin S 1992 *Solid State Commun.* **84** 635
- [10] Schleger P, Casalta H, Hadfield R, Poulsen H F, von Zimmermann M, Andersen N H, Schneider J R, Liang Ruixing, Dosanjh P and Hardy W N 1994 *Physica C* **241** 103
- [11] Zubkus V E, Lapinskas S and Tornau E E 1990 *Physica C* **166** 472
Zubkus V E, Lapinskas S, Rosengren A and Tornau E E 1993 *Physica C* **206** 155
- [12] de Fontaine D, Ceder G and Asta M 1990 *Nature* **343** 544; 1991 *Physica C* **177** 106
- [13] Lapinskas S, Tornau E E, Schleger P and Rosengren A 1995 to be published
- [14] Alario-Franco M A, Chaillout C, Capponi J J, Chenavas J and Marezio M 1988 *Physica C* **156** 455
- [15] Krekels T, Shi T S, Reyes-Gasga J, Van Tendeloo G, Van Landuyt J and Amenlinckx S 1990 *Physica C* **167** 677
- [16] Sonntag R, Hohlwein D, Brückel T and Collin G 1991 *Phys. Rev. Lett.* **66** 1497
Hohlwein D 1994 *Materials and Crystallographic Aspects of High- T_c Superconductivity* ed E Kaldis (Dordrecht: Kluwer)
- [17] Wille L T, Berrera A and de Fontaine D 1988 *Phys. Rev. Lett.* **60** 1065
- [18] Tornau E E, Lapinskas S, Grigelionis G and Rosengren A 1993 *Phys. Rev. Lett.* **70** 3139
- [19] Tornau E E, Kundrotas P J, Lapinskas S and Rosengren A 1994 *Solid State Commun.* **91** 393
- [20] Goldman M, Burmester C P, Wille L T and Gronsky R 1994 *Phys. Rev. B* **50** 1337
- [21] Semenovskaya S and Khachatryan A G 1992 *Phys. Rev. B* **46** 6511
- [22] Parliński K, Heine V and E Salje K H 1993 *J. Phys.: Condens. Matter* **5** 497

- [23] Aligia A A, Bonadeo H and Garces J 1991 *Phys. Rev. B* **43**
- [24] Aligia A A, Garces J and Bonadeo H 1992 *Physica C* **190** 234
- [25] Aligia A A and Garces J 1994 *Phys. Rev. B* **49** 524
- [26] Sterne P E and Wille L T 1989 *Physica C* **162-164** 223
- [27] Udvardi L, Szunyogh L, Redinger J, Weinberger P and Pasturel A 1994 *Phil. Mag.* **69** 683
- [28] Aligia A A and Garces J 1993 *Solid State Commun.* **87** 363
Aligia A 1994 *Europhys. Lett.* **26** 153
- [29] de Fontaine D 1994 *Europhys. Lett.* **26** 155
- [30] Adelman D, Burmester C P, Wille L T, Sterne P A and Gronsky R J. *Phys.: Condens. Matter* **4** L585
- [31] Schwer H-J, Kaldis E, Karpinski J and Rossel C 1993 *Physica C* **211** 165
- [32] Zubkus V E, Lapinskas S and Tornau E E 1989 *Physica C* **159** 501
Grigelionis G, Lapinskas S, Rosengren A and Tornau E E 1995 *Physica C* **242** 183
- [33] Zhao Z H, Zhou X J, Li J Q and Yao Y S 1994 *Physica C* **229** 35